Electron. Mater. Lett., Vol. 13, No. 4 (2017), pp. 359-367
DOI: 10.1007/s13391-017-6219-1

Performance Enhancement of Quantum Dot Sensitized Solar Cells under TiO_2 Nanotube Arrays Membranes Optimization

Zhuoyin Peng[1,*], Yueli Liu[2], Yinghan Zhao[2], Lida Liao[1], and Jian Chen[1]

[1]School of Energy and Power Engineering, Changsha University of Science and Technology, Changsha 410111, China
[2]State Key Laboratory of Advanced Technology for Materials Synthesis and Processing, and School of Materials Science and Engineering, Wuhan University of Technology, Wuhan 430070, China

(received date: 9 July 2016 / accepted date: 27 November 2016 / published date: 10 July 2017)

One-dimensional single crystalline TiO_2 nanotube arrays with different length are prepared, and transferred onto the FTO glass substrate with different concentration of Ti-precursor. The relationships between the concentration of Ti-precursor and the optical properties, as well as the photovoltaic performance of the as-prepared solar cells have been investigated. The optical absorption intensity is obviously enhanced and optical absorption edge is expanded to 800 nm for the CdSe/CdS/TiO_2 NTs solar cells. In addition, 20 μm - CdSe/CdS/TiO_2 NTs solar cells with 0.1 M Ti-precursor have the great photovoltaic conversion efficiency of 4.18%. The excellent photovoltaic performance is attributed to the suitable TiO_2 connection layer from 0.1 M Ti-precursor and length of TiO_2 NTs, which greatly enhances the electron-hole generation and charge transfer performance in the solar cells. Finally, the photovoltaic efficiency of the as-fabricated solar cells can be further enhanced to 4.51% through the ZnS passivation layer deposition.

Keywords: CdSe/CdS quantum dots sensitized solar cells, TiO_2 nanotube arrays, concentration of Ti-precursor, length of TiO_2 nanotubes, photovoltaic performance enhancement

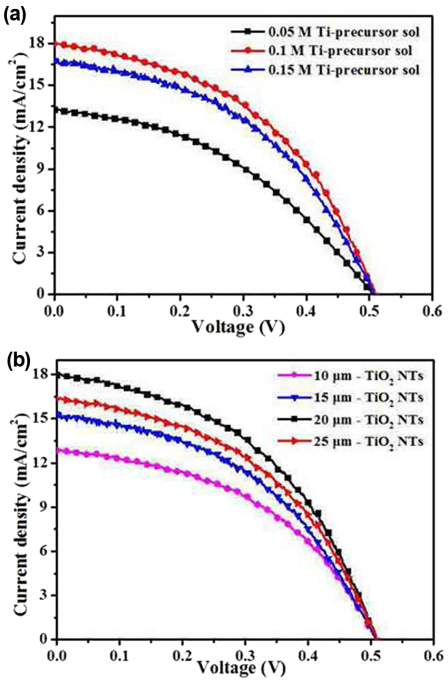

1. INTRODUCTION

Since the semiconductor quantum dots (QDs) been discovered, its unique properties of tunable band gap, high absorption coefficient, ultrafast electron transfer, quantum dots size-effect and multiple exciton generation have been widely employed to fabricate different kinds of optical-electronic devices.[1-7] Recently, quantum dot sensitized solar cells (QDSSCs) have become an important research area for the next generation photovoltaic devices. Various kinds of QDs such as CdX (X=S, Se, Te), PbX (X=S, Se, Te), $CuInX_2$ (X=S, Se), *et al.* have been investigated to improve the photovoltaic efficiency of QDSSCs.[8-10] In recent researches, it is found that PbX (X=S, Se, Te) and $CuInX_2$ (X=S, Se) system QDs have the great ultraviolet and visible light absorption properties, which can be employed for fabricating the excellent photovoltaic devices.[11,12] Due to the excellent optical properties of CdX (X=S, Se, Te) based QDs, the better photovoltaic performance have been obtained by

*Corresponding author: joeypengzy@outlook.com

optimize CdSe/CdS quantum dot sensitized solar cells.[13] However, the photovoltaic performance of these QDSSCs still needs to be improved. Therefore, it is still important for the further investigations on the CdSe/CdS QDSSCs to achieve a better photovoltaic efficiency.

In addition to QDs, the materials and structure of the basic photo-electrode also play an important role in QDSSCs. Traditionally, TiO_2 nanoparticle films have been employed as be the photo-electrodes of QDSSCs. However, the loss of the electrons at the grain boundaries in the TiO_2 nanoparticle films is inevitable, which will induce the electron-hole recombination in the solar cell system.[14] Therefore, many investigations have been focused on the one-dimensional single crystalline nanostructure to enhance the performance of the charge transfer, such as TiO_2 nanorods (NRs), nanowires (NWs) and nanotubes (NTs).[15-17] For comparison, TiO_2 NTs have larger surface area, and the unique tube structure can provide large area for QDs deposition, which would lead to better excellent photovoltaic performance. In traditional preparations, TiO_2 NTs are prepared on the non-transparent substrates, which can not illuminate from the back side. In order to solve this problem, the TiO_2 NTs have been detached as the membranes from the non-transparent substrates to transfer onto the transparent substrates for solar cells.[18] However, the structure and combination of the photo-electrodes still influence the photovoltaic performance of the QDSSCs. Therefore, it is significantly important to optimize the nanostructure of the TiO_2 NTs photo-electrodes in the QDSSCs system.

Herein, the TiO_2 NTs arrays were firstly prepared on the Ti substrate by anodization process, then transferred onto the FTO conducting glass through the TiO_2 sol. CdSe/CdS QDs were deposited on the TiO_2 NTs arrays by the successive ionic layer absorption and reaction (SILAR) process. The optimizations of the QDSSCs with different concentration of TiO_2 sol and length of TiO_2 NTs had been investigated to obtain the better photovoltaic performance of the QDSSCs.

2. EXPERIMENTAL PROCEDURE

2.1 Preparation of TiO_2 NTs arrays electrodes

TiO_2 NTs arrays were prepared on the FTO conducting glass by two-step process. Firstly, TiO_2 NTs arrays were prepared by the traditional anodization process on Ti substrate in the electrolyte consisting of 0.75 wt% distilled (DI) water and 0.25 wt% ammonium fluoride (NH_4F) in ethylene glycol (EG) at 60 V for 2-6 h (As shown in Fig. 1a and Fig. 1b). The different length of TiO_2 NTs was prepared with different anodization time. Afterward, the as-prepared samples were washed with DI water and ethanol to remove the impurities. Then the samples were dried at 80 °C before annealed at 500 °C for 1 h with the heating rate of 1 °C/min at ambient condition. Secondly, the annealed samples were anodized in the same fresh electrolyte at 60 V for another 30 min and washed with DI water. Whereafter, 10 wt% H_2O_2 solution was employed to detach the TiO_2 NTs array membranes from Ti substrate by putting the as-prepared samples into this solution for a few minutes (As shown in Fig. 1c). Then the TiO_2 NTs array membranes were adhered on the FTO conducting glass through a drop of TiO_2 sol consisting of titanium (IV) isopropoxide ethanol solution with different concentration of 0.05 M, 0.1 M and 0.15 M (As shown in Fig. 1d). After dried at 80 °C, the samples were annealed at 500 °C for 1h with the heating rate of 1 °C/min at ambient condition again to form the TiO_2 NTs arrays electrode.

2.2 Fabrication of CdSe/CdS QDs sensitized TiO_2 NTs solar cells

CdSe/CdS QDs were deposited on TiO_2 NTs electrodes by

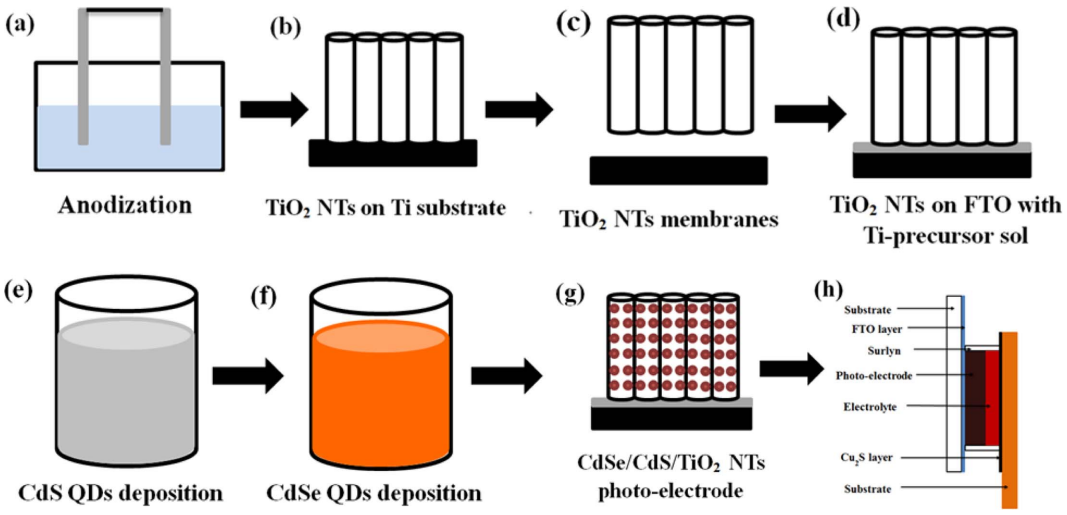

Fig. 1. Schematic of the preparation and fabrication of QDSSCs.

SILAR process (As shown in Fig. 1e and Fig. 1f). Typically, the as-prepared TiO_2 NTs electrodes were firstly immersed into a 0.1 M $Cd(NO_3)_2$ aqueous solution for 1 min following by distilled water washing for 1 min. And then the TiO_2 NTs electrodes were immersed in a 0.1 M Na_2S aqueous solution for 1 min following by distilled water washing for 1 min. This process was considered as one immersing cycle of SILAR procedure, which was introduced for 5 cycles to deposit CdS QDs. CdSe QDs were deposited on the prepared CdS/TiO_2 NTs electrodes by the similar process. The prepared CdS/TiO_2 NTs electrodes were firstly immersed into a 0.05 M $Cd(NO_3)_2$ aqueous solution for 1 min following by distilled water washing for 1 min. And then the TiO_2 NTs electrodes were immersed in a 0.05 M $NaSeH_4$ aqueous solution (SeO_2 into $NaBH_4$ aqueous solution under Ar atmosphere) for 1 min following by distilled water washing for 1 min. This process was considered as one immersing cycle of SILAR procedure, which was introduced for 11 cycles to deposit CdSe QDs. And the ZnS passivation layer was introduced by twice SILAR cycles in 0.1 M $Zn(NO_3)_2$ and 0.1 M Na_2S solution for 1 min per immerse, respectively. A Cu_2S films were prepared on the brass substrate as previous chemical reaction.[19] Then the QDSSCs were fabricated with the CdSe/CdS/TiO_2 NTs electrodes and Cu_2S/brass electrodes by using a thin transparent surlyn thermoplastic frame. A methanol/distilled water (7:3 by volume) solution containing 0.5 M Na_2S, 2 M S, and 0.2 M KCl was prepared as redox polysulfide electrolyte to inject into the sealed solar cells (As shown in Fig. 1h). The whole preparation process of QDSSCs was according to the schematic in Fig. 1.

2.3 Characterization and measurements

The scanning electron microscope (FESEM, JSEM-5610LV, Japan) were employed to characterize the morphologies of the electrodes. UV-vis absorption spectra (UV-2550, Shimadzu, Japan) were used to characterize the optical absorption properties enhancement of the electrodes. The photocurrent-voltage (*J-V*) curves were measured by the Keithley 4200 semiconductor characterization system (Keithley Instruments, USA) under AM 1.5 illumination (Newport 91160, 300 W xenon lamp, USA). The electrochemical impedance spectra (EIS) were measured by using an impedance analyzer (Auto lab PGSTAT320N) at open-circuit potentials under AM 1.5 illumination. The incident photon to current conversion efficiency (IPCE) was measured using Newport's IPCE Measurement Kit, where a monochromator was used to obtain the monochromatic light from a 300W Xe lamp (Newport).

3. RESULTS AND DISCUSSION

3.1 Structures and morphologies of CdSe/CdS/TiO_2 NTs electrodes

The TiO_2 NTs were prepared by anodization process and then transferred onto the FTO glass substrates. And then,

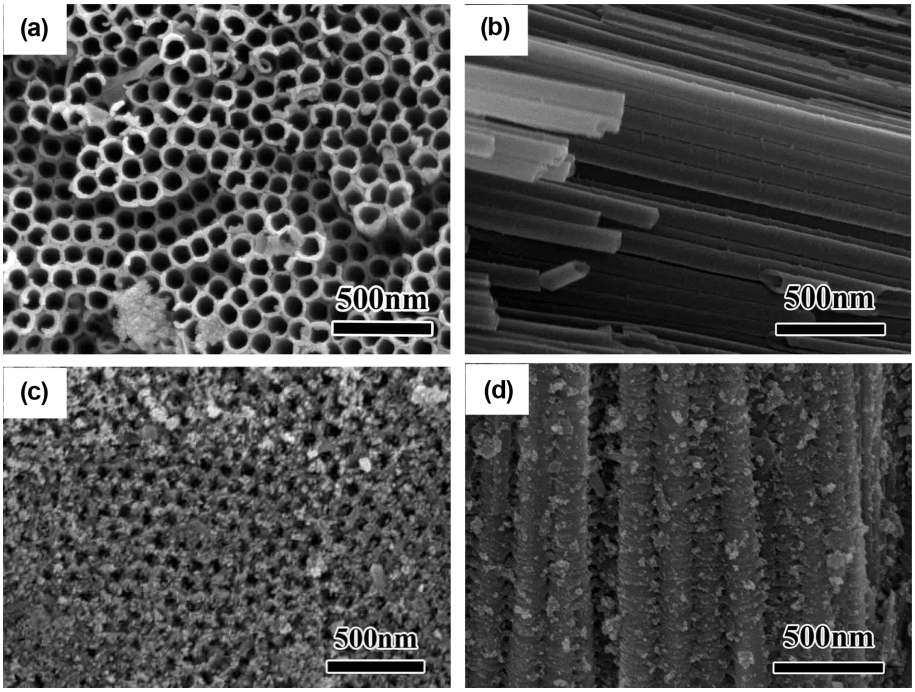

Fig. 2. FESEM images of pure TiO_2 NTs and CdSe/CdS/TiO_2 NTs photo-electrodes: (a) top-view of pure TiO_2 NTs, (b) corss-sectional of pure TiO_2 NTs, (c) top-view of CdSe/CdS/TiO_2 NTs and (d) cross-senctional of CdSe/CdS/TiO_2 NTs.

CdS and CdSe QDs were deposited on the TiO_2 NTs/FTO electrodes through the SILAR approach. Figure 2 shows the top-view and cross-sectional FESEM images of TiO_2 NTs and CdSe/CdS/TiO_2 NTs electrodes. An uniform tube structure with the average diameter of 100 nm and wall thickness of 10 nm can be clearly observed from the top-view FESEM image of pure TiO_2. Moreover, the cross-sectional image reveals the smooth and uniform vertial alignment structure of pure TiO_2. After QDs deposition, the diameter of nanotube decreased, which indicated that CdS and CdSe QDs have covered on the surface of TiO_2 NTs in the top-view FESEM image (Fig. 2c). In addtion, in cross-sectional FEM image (Fig. 2d), it can be seen that QDs are also deposited on the surface of nanotube, which reveals the inner deposition of QDs in the TiO_2 nanotube.

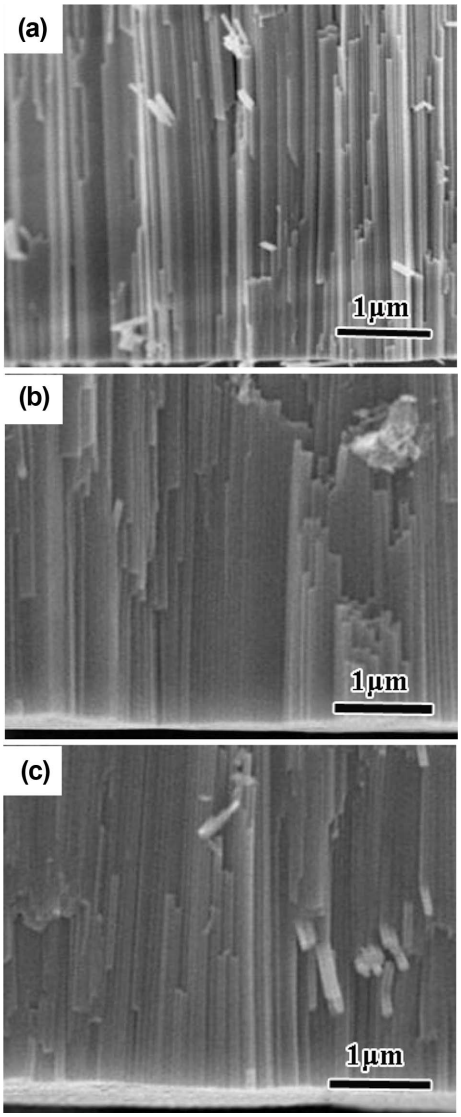

Fig. 3. FESEM images of CdSe/CdS/TiO_2 NTs photo-electrodes with different concentration of Ti-precursor: (a) 0.05 M, (b) 0.1 M and (c) 0.15 M.

3.2 Influence of sol concentration in CdSe/CdS/TiO_2 NTs solar cells

The originate TiO_2 NTs are prepared on the surface of Ti substrates, which are transferred and adhered onto the surface of FTO glass substrates with the Ti-precursor sol. Therefore, the concentration of Ti-precursor sol will seriously influence the connection between TiO_2 NTs and FTO substrates. Here, various concentrations of Ti-precursor sol containing 0.05 M, 0.1 M and 0.15 M are investigated to optimize the performance of CdSe/CdS/TiO_2 NTs photo-electrodes by employing the 20 μm – TiO_2 NTs. Figure 3 shows the FESEM images of CdSe/CdS/TiO_2 NTs photo-electrodes with different concentration of Ti-precursor sol, which can be found that the thickness of TiO_2 nanoparticle connection layer gradually increase. As shown in Fig. 3a, it can be doubted that the TiO_2 nanoparticle layer from 0.05 M Ti-precursor sol can not form well connection of TiO_2 NTs and FTO substrate. To the contrary, the TiO_2 nanoparticle layer from 0.1 M and 0.15 M Ti-precursor sol have

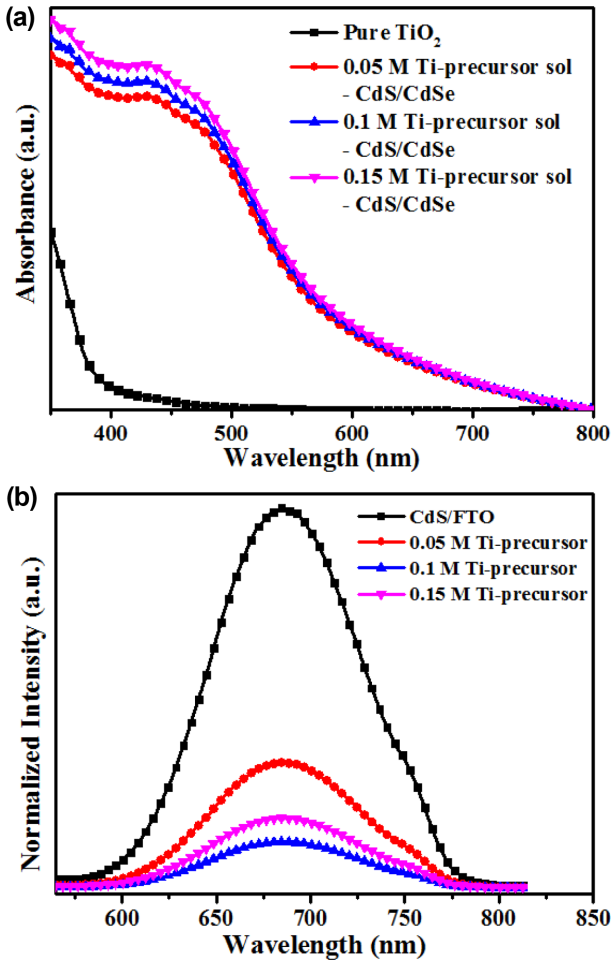

Fig. 4. Different concentration of Ti-precursor: (a) UV-vis absorption spectra of CdSe/CdS/TiO_2 NTs photo-electrodes and (b) Normalized PL spectra of CdSe/CdS/TiO_2 NTs photo-electrodes.

considerable thickness for the connection of TiO_2 NTs and FTO substrate, respectively. Therefore, relatively suitable concentration of Ti-precursor sol is very important.

Figure 4a shows the UV-vis absorption spectra of CdSe/CdS/TiO_2 NTs photo-electrodes with different concentration of Ti-precursor sol. Different from low optical absorption edge of pure TiO_2 NTs, the ultraviolet and visible light absorption edge of all three different CdSe/CdS/TiO_2 NTs photo-electrodes have greatly enhanced from 400 nm to 800 nm. And almost no distinction has been observed for the absorption edge of all these three CdSe/CdS/TiO_2 NTs photo-electrodes. However, the optical absorption intensities of the photo-electrodes are gradually increased with the concentration increasing of Ti-precursor sol. As we know, the Ti-precursor sol will form a TiO_2 nanoparticle layer on the FTO glass substrates after heat-treatment, which means that the concentration increasing of Ti-precursor sol will lead to the increasing of the thickness of TiO_2 nanoparticle layer. This may provide more carriers for the QDs deposition, inducing the enhancement of optical absorption property.

In order to observe the electron-hole separation and recombination property, CdS QDs sensitized TiO_2 NTs photo-electrodes are employed to analyze the normalized PL spectra of three different photo-electrodes in Fig. 4b. The PL peaks of CdS/FTO and three different CdS/TiO_2 NTs photo-electrodes are at the approximate wavelength of 560 nm, which indicates that different concentration of Ti-precursor sol have no effect on the PL performance of photo-electrodes. Comparing with the CdS/FTO photo-electrode, the normalized PL intensities of three different CdS/TiO_2 NTs photo-electrodes have obviously quenched, indicating the effective electron-hole separation in the CdS/TiO_2 NTs photo-electrodes system. Moreover, the normalized PL intensity of CdS/TiO_2 NTs photo-electrodes with 0.1 M Ti-precursor sol is much lower than that of 0.05 M and 0.15 M, which means that the CdS/TiO_2 NTs photo-electrodes with 0.1 M Ti-precursor sol has the best electron-hole separation property. In these three concentrations of Ti-precursor sol, the thickness of TiO_2 layer from 0.05 M Ti-precursor sol may be not enough for the well connection between TiO_2 NTs and FTO glass substrate, inducing the electron-hole recombination. Meanwhile, the thickness of TiO_2 layer from 0.15 M Ti-precursor sol may be too much, which will provide more barriers from grain boundaries between nanoparticles inducing the electron-hole recombination. Therefore, only employing suitable concentration 0.1 M Ti-precursor sol for the TiO_2 layer can obtain the best electron-hole separation performance.

In order to investigate the photovoltaic performance of the QDSSCs fabricated through various concentrations of Ti-precursor sol, the *J-V* curves and photovoltaic parameters of the three different CdSe/CdS/TiO_2 NTs solar cells are shown in Fig. 5a and Table 1. There is no obvious distinction of open-circuit voltage (V_{OC}) value for three different CdSe/CdS/TiO_2 NTs solar cells (508.7 mV, 508.6 mV and 508.3 mV), indicating nothing changes for the negative potential in Fermi level of photo-electrodes under different

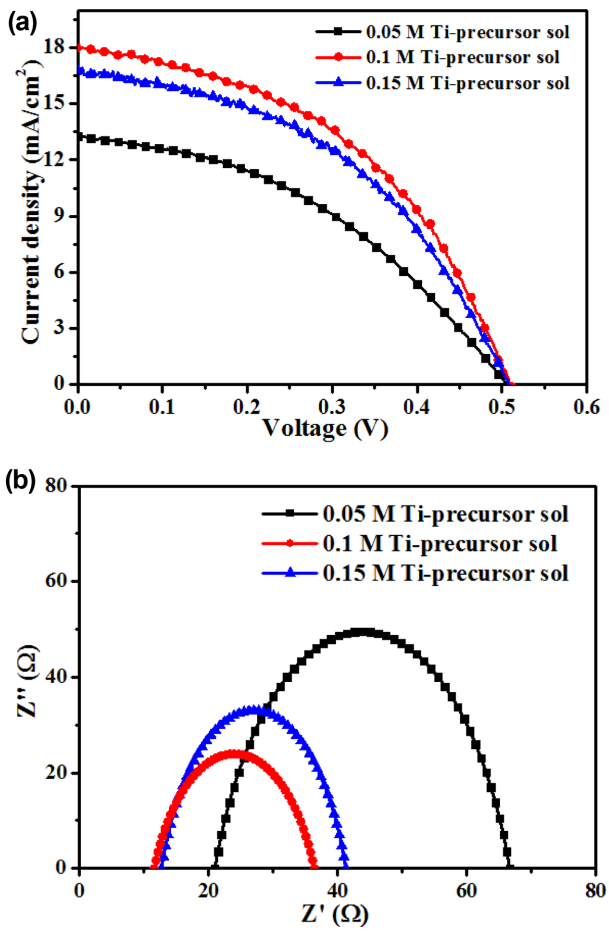

Fig. 5. Different concentration of Ti-precursor: (a) J-V curves of CdSe/CdS/TiO_2 NTs solar cells and (b) EIS plots of CdSe/CdS/TiO_2 NTs solar cells.

Table 1. Photovoltaic and EIS parameters of the QDSSCs with different concentration of Ti-precursor.

Ti-precursor Concentration	V_{OC} (mV)	J_{SC} (mA/cm^2)	*FF* (%)	η (%)	R_s (Ω)	R_{CT} (Ω)
0.05 M	508.7	13.31	40.2	2.86	21.1	45.3
0.1 M	508.6	17.96	45.8	4.18	11.7	24.5
0.15 M	508.3	16.55	46.7	3.92	12.8	28.4

concentration of Ti-precursor sol. However, the fill factor (*FF*) and short-circuit current density (J_{SC}) of 0.05 M Ti-precursor based CdSe/CdS/TiO_2 NTs solar cells are 0.402 and 13.31 mA/cm^2, which is obviously lower than that of 0.1 M and 0.15 M Ti-precursor sol based solar cells. Due to the low concentration of Ti-precursor (0.05 M), the negative connection between TiO_2 NTs and FTO glass substrate may be formed which will increase the series resistance and possibility of electron-hole recombination in photo-electrodes to reduce the *FF* and J_{SC} of solar cells. Comparing with QDSSCs prepared by 0.1 M and 0.15 M Ti-precursor sol, the more stable connection between TiO_2 NTs and FTO glass substrate by 0.15 M Ti-precursor sol provides the slightly higher *FF* of the solar cells (0.467) than that of 0.1 M Ti-precursor sol (0.458). However, 0.1 M Ti-precursor sol based CdSe/CdS/TiO_2 NTs solar cell has the higher J_{SC} value of 17.96 mA/cm^2. The relatively large thickness of TiO_2 layer by 0.15 M Ti-precursor sol will produce much more TiO_2 nanoparticles in the photo-electrodes system. The gain boundaries between those nanoparticles will produce more barriers to prevent the charge transfer of the solar cells. Therefore, the 0.1 M Ti-precursor sol based CdSe/CdS/TiO_2 NTs solar cell has the better photovoltaic conversion efficiency of 4.18%.

To further clarify the electron transfer performance of different Ti-precursor sol based CdSe/CdS/TiO_2 NTs solar cells, the resistance values of photo-electrodes are determined by EIS measurement in Fig. 5b and Table 1. The series resistance (R_s) of 0.1 M and 0.15 M Ti-precursor sol based CdSe/CdS/TiO_2 NTs photo-electrodes are obviously lower than that of 0.05 M Ti-precursor sol, which can demonstrate the unfavorable connection in 0.05 M Ti-precursor sol based CdSe/CdS/TiO_2 photo-electrodes and stability enhancement of CdSe/CdS/TiO_2 photo-electrodes with concentration increasing of Ti-precursor sol, further inducing the change of *FF* value for solar cells. Moreover, with the concentration increasing of Ti-precursor sol, the charge transfer resistances (R_{CT}) of CdSe/CdS/TiO_2 NTs photo-electrodes first increase and then decrease which match well with PL spectra in Fig. 4b. In photo-electrode systems, the unfavorable connection from 0.05 M Ti-precursor sol will reduce the path of electron transfer, and relatively excessive nanoparticles from 0.15 M Ti-precursor will induce the gain boundaries, which both increase the possibility of electron-hole recombination. On the contrary, the 0.1 M Ti-precursor sol based CdSe/CdS/TiO_2 NTs photo-electrodes not only provide stable connection for TiO_2 NTs and FTO glass substrate, but also introduce the relatively less barriers for charge transfer, finally obtaining the lowest R_s value of 11.7 Ω and R_{CT} value of 24.5 Ω. Therefore, employing the concentration of 0.1 M Ti-precursor sol can enhance the photovoltaic performance of CdSe/CdS/TiO_2 NTs solar cells.

3.3 Length influence of nanotube in CdSe/CdS/TiO_2 NTs solar cells

The thickness of thin film influences the optical property and photovoltaic performance of QDSSCs. Here the length of TiO_2 NTs (containing of 10 μm, 15 μm, 20 μm and 25 μm) have been investigated in CdSe/CdS/TiO_2 NTs solar cells by employing 0.1 M Ti-precursor sol. In Fig. 6a, with the approximate optical absorption edges, it can be seen that the UV-vis absorption intensity of CdSe/CdS/TiO_2 NTs photo-electrodes are gradually enhanced with the length increasing of TiO_2 NTs. However, the UV-vis absorption intensity of 25 μm - CdSe/CdS/TiO_2 NTs photo-electrode is slightly higher than that of 20 μm, which can be assumed that the prolonged 5 μm of TiO_2 NTs is unnecessary for the optical absorption. Fig. 6b shows the normalized PL spectra of CdS/TiO_2 NTs photo-electrodes with different length of TiO_2 NTs. Comparing with pure CdS/FTO electrodes, the normalized PL peaks of all the CdS/TiO_2 NTs photo-electrodes are obviously quenched to the approximate PL

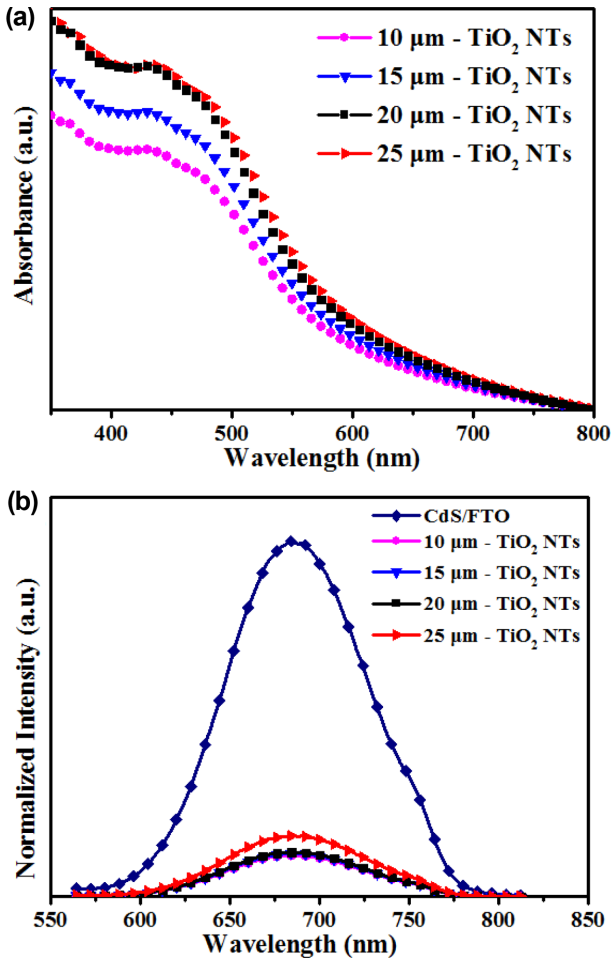

Fig. 6. Different length of TiO_2 NTs: (a) UV-vis absorption spectra of CdSe/CdS/TiO_2 NTs photo-electrodes and (b) Normalized PL spectra of CdSe/CdS/TiO_2 NTs photo-electrodes.

intensity except 25 μm - CdS/TiO_2 NTs photo-electrode. The PL intensity of 25 μm - CdS/TiO_2 NTs photo-electrode is higher than other length of TiO_2 NTs, which may be attributed to the relatively excessive length of TiO_2 NTs to increase the possibility of electron-hole recombination. Therefore, it can be considered that the 20 μm - CdSe/CdS/TiO_2 NTs photo-electrode may be better to obtain excellent photovoltaic performance of the solar cells.

The *J-V* curves, EIS plots and photovoltaic parameters are measured in Fig. 7 and Table 2. There have approximate V_{OC} and *FF* values for all the CdSe/CdS/TiO_2 NTs solar cells with different length of TiO_2 NTs, as well as the similar results for the R_s values of CdSe/CdS/TiO_2 NTs photo-electrodes. For comparison, the J_{SC} values of CdSe/CdS/TiO_2 NTs solar cells first increase then decrease with the length increasing of TiO_2 NTs, which have the highest J_{SC} value of 17.96 mA/cm^2 at the length of 20 μm. With the length increasing of TiO_2 NTs, the quantity of QDs deposition are gradually increased, which can provide much more photo-induced electrons for the photo-electrodes to improve the current density of the solar cells. However, although the 25 μm - CdSe/CdS/TiO_2 NTs photo-electrode

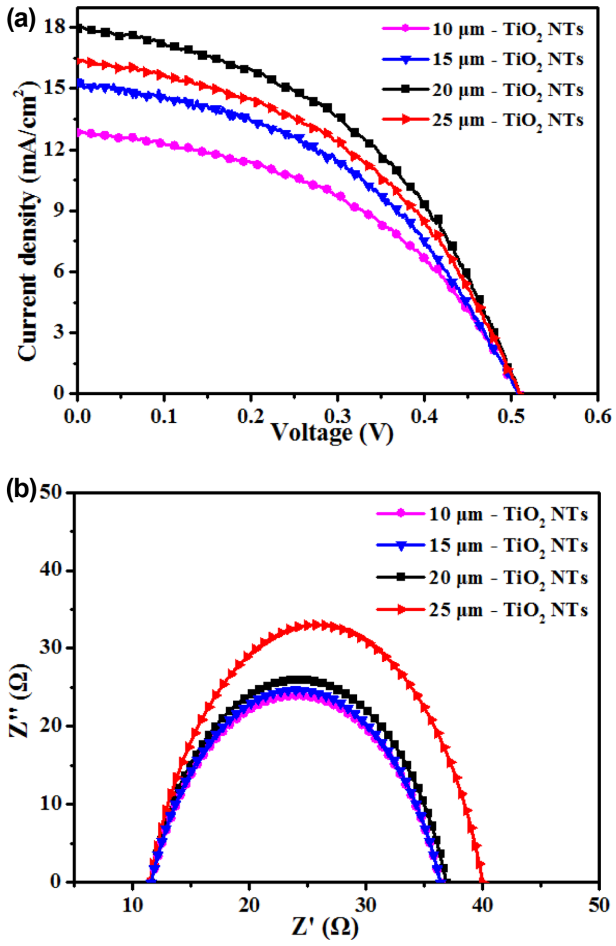

Fig. 7. Different length of TiO_2 NTs: (a) *J-V* curves of CdSe/CdS/TiO_2 NTs solar cells and (b) EIS plots of CdSe/CdS/TiO_2 NTs solar cells.

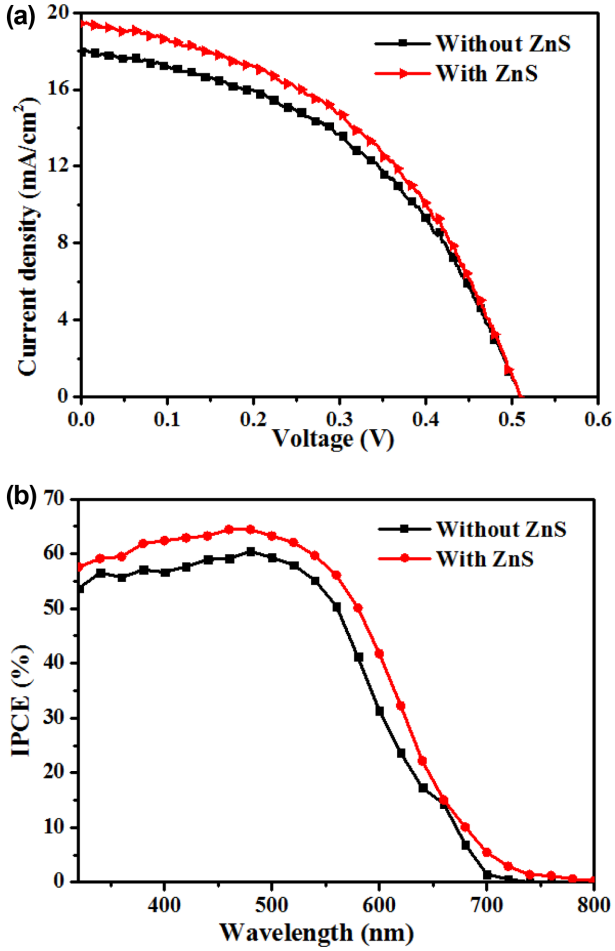

Fig. 8. With ZnS passivaition layer: (a) *J-V* curves of CdSe/CdS/TiO_2 NTs solar cells; (b) IPCE spectra of CdSe/CdS/TiO_2 NTs solar cells.

Table 2. Photovoltaic and EIS parameters of the QDSCs with different length of TiO_2 NTs.

Length of TiO_2 NTs	V_{OC} (mV)	J_{SC} (mA/cm^2)	*FF* (%)	η (%)	R_s (Ω)	R_{CT} (Ω)
10 μm	508.3	12.84	45.6	2.97	11.4	23.7
15 μm	508.2	15.31	45.2	3.54	11.5	23.9
20 μm	508.6	17.96	45.8	4.18	11.7	24.5
25 μm	509.1	16.35	45.5	3.78	11.6	28.6

have excellent optical absorption property, some part of relatively excessive length of 25 μm - CdSe/CdS/TiO_2 NTs photo-electrode may not capture photon to generate electron-holes, which will become the barrier of charge transfer and center of charge recombination in the solar cells to decrease the J_{SC} value (16.35 mA/cm^2). Therefore, due to the advantages of charge generation and transfer performance, higher J_{SC} value can be obtained by 20 μm - CdSe/CdS/TiO_2 NTs solar cells. Furthermore, the R_{CT} values of CdSe/CdS/TiO_2 NTs photo-electrodes have the similar tendency of J_{SC} values. The R_{CT} values of 10 μm, 15 μm and 20 μm - CdSe/CdS/TiO_2 NTs photo-electrode have slightly increased (23.7 Ω, 23.9 Ω and 24.5 Ω), which indicates that there have few effect for the charge transfer performance of these three photo-electrodes with the length increasing of TiO_2 NTs. However, the R_{CT} value of the 25 μm - CdSe/CdS/TiO_2 NTs photo-electrode is obviously higher than that of three photo-electrodes, which can be believed the barrier of charge transfer in the relatively long length of TiO_2 NTs. Those results demonstrate that the 20 μm - CdSe/CdS/TiO_2 NTs photo-electrodes can provide better photovoltaic performance of solar cells.

After the optimizations of the photo-electrode, the 20 μm - CdSe/CdS/TiO_2 NTs solar cells with 0.1 M Ti-precursor have received the photovoltaic conversion efficiency of 4.18%. In order to further enhance photovoltaic efficiency of the solar cells, the traditional ZnS passivation layer is prepared on the surface of CdSe/CdS/TiO_2 NTs photo-electrodes. In Fig. 8a, with nothing influence for the V_{OC} and *FF* values, it can be seen that the J_{SC} values have obviously enhanced after the ZnS passivation layer deposition, final indicating the photovoltaic efficiency to 4.51%. And the IPCE spectra of CdSe/CdS/TiO_2 NTs solar cells Fig. 8b cover the whole optical wavelength of 300-800 nm, which match well with the UV-vis absorption spectra in Fig. 4a. And the IPCE value of the CdSe/CdS/TiO_2 NTs solar cells with ZnS passivation layer is higher than that of prue CdSe/CdS/TiO_2 NTs solar cells, which can support the photovoltaic performance enhancement in the whole ultraviolet and visible light region.

4. CONCLUSIONS

In summary, the CdSe/CdS/TiO_2 NTs solar cells have been successfully prepared on the FTO glass substrates, and concentration of Ti-precursor and length of TiO_2 NTs have been optimized to enhance the performance of the as-fabricated solar cells. The charge transfer and photovoltaic performance of 0.1 M Ti-precursor based CdSe/CdS/TiO_2 NTs solar cells are obviously improved, which is due to the barrier of charge transfer from the relatively low concentration of 0.05 M and high concentration of 0.15 M Ti-precursor. With the concentration of 0.1 M Ti-precursor, the 20 μm - CdSe/CdS/TiO_2 NTs solar cells have the best photovoltaic performance, which is attributed to the relatively higher optical absorption property and lower possibility of electron-hole recombination from suitable length of TiO_2 NTs. After the ZnS passivation layer deposition, the optimized CdSe/CdS/TiO_2 NTs solar cells have received the excellent photovoltaic efficiency of 4.51%. It can be believed that TiO_2 NTs arrays can effectively instead nanoparticles for excellent photovoltaic devices by this process.

ACKNOWLEDGEMENT

This work is supported by the National Nature Science Foundation of China (No. 11674258), the Key project of science and technology plan of Hunan Province (2015WK3023), Science and Technology Support Program of Hubei Province (No. 2014BAA096), the Reserch Foundation of Education Bureau of Hunan Province (Grant No.17C0025), the Key Laboratory of Optoelectronic Devices and Systems of Ministry of Education and Guangdong Province (No. GD201402) and the Key Laboratory of Efficient & Clean Energy Utilization, The Education Department of Hunan Province (No. 2017NGQ007). Thanks for the measurements supporting from Center for Materials Research and Analysis at Wuhan University of Technology (WUT).

REFERENCES

1. M. R. Bergren, P. K. Palomaki, N. R. Neale, T. E. Furtak, and M. C. Beard, *ACS Nano*. **10**, 2316 (2016).
2. M. Molaei, H. Hasheminejad, and M. Karimipour, *Electron. Mater. Lett.* **11**, 7 (2015).
3. J. Du, Z. L. Du, J. S. Hu, Z. X. Pan, Q. Shen, J. K. Sun, D. H. Long, H. Dong, L. T. Sun, X. H. Zhong, and L. J. Wan, *J. Am. Chem. Soc.* **138**, 4201 (2016).
4. T. Debnath, P. Maity, T. Banerjee, A. Das, and H. N. Ghosh, *J. Phys. Chem. C* **119**, 3522 (2015).
5. G. H. Carey, A. L. Abdelhady, Z. J. Ning, S. M. Thon, O. M. Bakr, and E. H. Sargent, *Chem. Rev.* **115**, 12732 (2015).
6. I. Jang, J. W. Kim, C. J. Park, C. Ippert, T. Greco, M. S. Oh, J. G. Lee, W. K. Kim, A. Wedel, C. J. Han, and S. K. Park, *Electron. Mater. Lett.* **11**, 1066 (2015).
7. X. W. Gong, Z. Y. Yang, G. Walters, R. Comin, Z. J. Ning, E. Beauregard, V. Adinolfi, O. Voznyy, and E. H. Sargent, *Nature Photon.* **10**, 253 (2016).
8. N. Y. Tam, N. Y. Truong, and C. H. Park, *Electron. Mater. Lett.* **12**, 308 (2016).
9. M. X. Liu, F. P. Arquer, Y. Y. Li, X. Z. Lan, G. H. Kim, O. Voznyy, L. K. Jagadamma, A. S. Abbas, S. Hoogland, Z. H. Lu, J. Y. Kim, A. Amassian, and E. H. Sargent, *Adv. Mater.* **28**, 4142 (2016).
10. Z. Y. Peng, Y. L. Liu, Y. H. Zhao, K. Q. Chen, Y. Q. Cheng,

and W. Chen, *Electrochim. Acta* **135**, 276 (2014).
11. X. Z. Lan, O. Voznyy, A. Kiani, F. P. Arquer, A. S. Abbas, G. H. Kim, M. X. Liu, Z. Y. Yang, G. Walters, J. X. Xu, M. J. Yuan, Z. J. Ning, F. J. Fan, P. Kanjanaboos, I. Kramer, D. Zhitomirsky, P. Lee, A. Perelgut, S. Hoogland, and E. H. Sargent, *Adv. Mater.* **28**, 299 (2016).
12. Z. Y. Peng, Y. L. Liu, K. Q. Chen, G. J. Yang, and W. Chen, *Chem. Eng. J.* **244**, 335 (2014).
13. Z. W. Ren, J. Wang, Z. X. Pan, K. Zhao, H. Zhang, Y. Li, Y. X. Zhao, I. M. Sero, J. Bisquert, and X. H. Zhong, *Chem. Mater.* **27**, 8398 (2015).
14. J. H. Im, J. S. Luo, M. Franckevičius, N. Pellet, P. Gao, T. Moehl, S. M. Zakeeruddin, M. K. Nazeeruddin, M. Grätzel, and N. G. Park, *Nano Lett.* **15**, 2120 (2015).
15. Z. Y. Peng, Y. L. Liu, Y. H. Zhao, W. Shu, K. Q. Chen, Q. L. Bao, and W. Chen, *Electrochem. Acta* **111**, 755 (2013).
16. C. Ngangham, A. Mondal, and B. Choudhuri, *Electron. Mater. Lett.* **11**, 758 (2015).
17. Z. C. Lian, W. C. Wang, S. N. Xiao, X. Li, Y. Y. Cui, D. Q. Zhang, G. S. Li, and X. Li, *Sci. Rep.* **5**, 10461 (2015).
18. C. S. Kim, S. H. Kim, J. H. Lee, J. Y. Kim, and J. Y. Yoon, *ACS Appl. Mater. Interfaces* **7**, 7486 (2015).
19. S. Gimenez, I. M. Sero, L. Macor, N. Guijarro, T. L. Villarreal, R. Gomez, L. J. Diguna, Q. Shen, T. Toyoda, and J. Bisquert, *Nanotechnology* **20**, 295204 (2009).